Dissipative structures in left-handed material cavity optics

Philippe Tassin,[a] Lendert Gelens,[b] Jan Danckaert,[c] Irina Veretennicoff,[d] and Guy Van der Sande[e]
Department of Applied Physics and Photonics, Vrije Universiteit Brussel, Pleinlaan 2, B-1050 Brussel, Belgium

Pascal Kockaert[f]
Optique et Acoustique, Université Libre de Bruxelles, CP 194/5, 50 Av. F. D. Roosevelt, B-1050 Bruxelles, Belgium

Mustapha Tlidi[g]
Optique Non Linéaire Théorique, Université Libre de Bruxelles, CP 231, Campus Plaine, B-1050 Bruxelles, Belgium

(Received 22 March 2007; accepted 11 July 2007; published online 28 September 2007)

We study the spatiotemporal dynamics of spatially extended nonlinear cavities containing a left-handed material. Such materials, which have a negative index of refraction, have been experimentally demonstrated recently, and allow for novel electromagnetic behavior. We show that the insertion of a left-handed material in an optical resonator allows for controlling the value and the sign of the diffraction coefficient in dispersive Kerr resonators and degenerate optical parametric oscillators. We give an overview of our analytical and numerical studies on the stability and formation of dissipative structures in systems with negative diffraction. © *2007 American Institute of Physics*. [DOI: 10.1063/1.2768158]

The formation of self-organized structures has been extensively investigated in various fields including biology, fluid mechanics, chemistry, laser physics, and nonlinear optics. In optical systems, localized structures have been proposed as basic objects for all-optical information transmission and processing. Diffraction plays an important role in the formation of optical patterns, and affects the typical size of these structures. In this contribution, we propose a scheme of diffraction control in optical nonlinear cavities filled with a left-handed material. These materials have a negative index of refraction, and have been demonstrated to exhibit extraordinary optical propagation properties, such as subwavelength resolution and electromagnetic cloaking. Here, we investigate the influence of introducing left-handed materials in two optical prototypes of dissipative nonlinear systems: a Kerr cavity containing a third-order nonlinearity, and a parametric oscillator containing a crystal with a second-order nonlinearity. We show that diffraction can be controlled by changing the relative amount of left-handed and right-handed materials in the cavity, and we study the formation of dissipative structures in these prototype systems with negative diffraction.

[a]Electronic mail: philippe.tassin@vub.ac.be
[b]Electronic mail: lendert.gelens@vub.ac.be
[c]Electronic mail: jan.danckaert@vub.ac.be
[d]Electronic mail: ivereten@vub.ac.be
[e]Electronic mail: guy.van.der.sande@vub.ac.be
[f]Electronic mail: pascal.kockaert@ulb.ac.be
[g]Electronic mail: mtlidi@ulb.ac.be

I. INTRODUCTION

Spatially extended systems support a large variety of dissipative structures, which can be either stationary or time-dependent. Their formation is attributed to the balance between the following phenomena: (i) a nonlinear mechanism, which typically involves chemical reactions or light-matter interaction, that tends to amplify spatial inhomogeneities; (ii) a transport process such as diffusion, thermal diffusivity, or diffraction that, on the contrary, tends to restore spatial uniformity; and (iii) dissipation. The spontaneous emergence of a dissipative pattern out of a homogeneous state was first predicted theoretically in the context of morphogenesis by Turing.[1] This symmetry-breaking instability is therefore called a Turing bifurcation. In most cases, the spatial patterns are intrinsic, i.e., the pattern's characteristic length (or wavelength) is determined by the dynamical parameters and not by geometrical constraints imposed by the boundary conditions. Self-organization and pattern formation is a well documented issue and has been observed in a variety of natural systems, such as in biology, reaction-diffusion processes, fluid mechanics, and nonlinear optics. A number of reviews can be found in Refs. 2–19. Laser physics and nonlinear optics provide examples of nonequilibrium systems that undergo instabilities accessible to experimental investigations. Driven nonlinear cavities filled with a nonlinear medium belong to this field and constitute the basic configurations in diffractive nonlinear optics. In these devices, the spatial coupling is provided by diffraction, which affects both the amplitude and the phase of light. When the Turing instability becomes subcritical, there exists a pinning region where localized spots of light become stable. Such light spots have attracted a lot of interest because of their potential applica-

tion as bits for information storage and processing. Different configurations have been proposed, such as two-level atomic systems,[20] systems with Kerr materials,[21–23] quadratic crystals,[24–27] semiconductors[28] or saturable absorbers,[29–31] and single mirror feedback systems.[32] The investigation of modulational instabilities is a prerequisite for the study of localized structures.

In recent years, there has also been considerable interest in left-handed materials and the concept of negative refraction. This concept was first suggested by Mandelstam,[33] and the fundamental properties of materials with simultaneously negative permittivity and permeability were explored by Veselago as early as 1968.[34] Nevertheless, it was only in 2001 that the first microwave left-handed material was demonstrated experimentally.[35] Generally, the special optical properties of these metamaterials are due to their artificial subwavelength structure. In the most common microwave metamaterial, split ring resonators providing negative permeability are combined with metallic wires providing negative permittivity,[36,37] although other geometries have been proposed. More recently, researchers from different groups have scaled down these structures to fabricate left-handed materials at optical wavelengths.[38–40] Metamaterials have been proposed for various applications, such as electromagnetic cloaking,[41,42] subwavelength imaging,[43] lenses with improved performance,[43–45] etc.

The novel properties of left-handed materials also have a dramatic impact when included in nonlinear optical systems. A first nonlinear left-handed material was proposed by Zharov *et al.*[46] The propagation of light in nonlinear left-handed materials was modeled theoretically,[47] and solitons were predicted in conservative systems with negative refractive index.[48] The fundamentals of second-harmonic generation have been considered in Refs. 49 and 50, resulting in the proposal of an opaque lens with subwavelength resolution.

In this paper, we want to investigate the influence of left-handed materials on the spatiotemporal dynamics of dissipative nonlinear optical systems. A huge variety of such systems exists, but we will consider here two prototype devices: a dispersive Kerr resonator containing a third-order nonlinearity, and a degenerate optical parametric oscillator containing a second-order nonlinearity. These simple systems will demonstrate how a left-handed material can alter the spatiotemporal dynamical behavior of dissipative structures. We first review the derivation of a propagation model for those systems, and its reduction to a mean-field model. We show quite generally that the insertion of a left-handed material in a ring cavity allows for the control of the total diffraction strength in a ring cavity. It is not only possible to alter the strength of diffraction, but also its sign can be changed by the left-handed material, leading to a regime of negative diffraction. We study the modulational stability of homogeneous output beams in this negative diffraction regime, and investigate the formation of dissipative structures with analytical and numerical techniques. We construct the branches of the dissipative patterns emerging from the modulational instability from a weakly nonlinear perturbation analysis, and we search numerically for stripes in the mean-field models of the considered systems. For the Kerr resonator, we find that the stability is altered dramatically, and that the process of pattern selection is dominated by a switching behavior induced in the bistable loop. For the degenerate optical parametric oscillator, we find periodic dissipative structures for positive detuning of the signal field.

II. PROPAGATION OF LIGHT IN NONLINEAR LEFT-HANDED MATERIALS

Before we start considering optical dissipative systems with left-handed materials, it is necessary to investigate the propagation of light in such materials. Traditionally, the propagation of optical signals in materials can be characterized by its refractive index n, which originates from the scattering of light by the atomic constituents of the material. The underlying reradiation processes induce an electric dipole density $\mathbf{P}$ given by

$$\mathbf{P}(\mathbf{r},t) = \epsilon_0 \int_{-\infty}^{\infty} \chi(t-\tau)\mathbf{E}(\mathbf{r},\tau)\mathrm{d}\tau, \tag{1}$$

where χ is the susceptibility related to the atomic polarizability and ϵ_0 is the permittivity of vacuum. The integral accounts for dispersion, i.e., the noninstantaneous response of the material. With the behavior of the optical material modeled by Eq. (1), Maxwell's equations can be reduced to a well-known propagation equation for the electric field $\mathbf{E}$,

$$-\nabla\times\nabla\times\mathbf{E}(\mathbf{r},t) - \frac{1}{c^2}\frac{\partial^2}{\partial t^2}\int_{-\infty}^{\infty}\epsilon_r(t-\tau)\mathbf{E}(\mathbf{r},\tau)\mathrm{d}\tau = \mu_0\frac{\partial^2}{\partial t^2}\mathbf{P}^{(\mathrm{NL})}(\mathbf{r},t), \tag{2}$$

with ϵ_r the relative permittivity, μ_0 the permeability of vacuum, and $\mathbf{P}^{\mathrm{NL}}$ the nonlinear part of the polarization field.

When considering coherent light signals with pulses longer than the wavelength (down to femtosecond pulses at optical wavelengths), the electric field can be represented by wave packets of the form

$$\mathbf{E} = \mathbf{A}(\mathbf{r},t)e^{i(\mathbf{k}\cdot\mathbf{r}-\omega t)} + \mathrm{c.c.}, \tag{3}$$

where the envelope $\mathbf{A}(\mathbf{r},t)$ evolves on a much slower time and space scale than the carrier at frequency ω and wave vector $\mathbf{k}$. Because of these large-scale differences and because the nonlinearity is a small contribution to the field evolution, a multiple scales perturbation technique can be applied to Maxwell's equations.[51] This leads to the following equation describing the field amplitude A of an optical signal propagating along the z axis:

$$\frac{\partial A}{\partial \xi} = \frac{\partial A}{\partial z} + \frac{n}{c}\frac{\partial A}{\partial t} = \frac{ic}{2\omega n}\nabla_\perp^2 A - \frac{i\beta}{2}\frac{\partial^2 A}{\partial t^2}, \tag{4}$$

where c is the velocity of light, n is the index of refraction, β is the group velocity dispersion coefficient, ξ is the longitudinal coordinate of a reference frame moving with the group velocity, and $\nabla_\perp^2 = \partial_x^2 + \partial_y^2$. Such propagation equations can be generalized to media with nonlinearities. For example, for a third-order—or Kerr—nonlinearity, one obtains the so-called nonlinear Schrödinger equation,[51,52]

$$\frac{\partial A}{\partial \xi} = \frac{ic}{2\omega n}\nabla_\perp^2 A - \frac{i\beta}{2}\frac{\partial^2 A}{\partial t^2} + \frac{i3\omega}{2cn}\chi^{(3)}|A|^2 A, \tag{5}$$

with $\chi^{(3)}$ the third-order susceptibility.

A similar analysis can be performed for the propagation of light in left-handed materials. The polarization field can still be described by Eq. (1), but one must keep in mind that the electric dipoles will now originate from the subwavelength structured units of the material rather than from individual atoms. The main difference in the above derivation comes from the fact that left-handed materials have intrinsically a strong magnetic behavior providing their negative permeability, and it is therefore not obvious that Eq. (5), which is derived for $\mu_r(\omega)=1$, can still describe the propagation of light in left-handed materials. Intuitively, one can expect that the knowledge of only the refractive index is not sufficient to describe the optical properties of such materials, since their electrodynamic behavior is characterized by two parameters: the permittivity ϵ_r and the permeability μ_r. The magnetic behavior of a left-handed material can be modeled by a constitutive equation analogous to Eq. (1), relating the volume density of magnetic dipoles $\mathbf{M}$ to the magnetic field $\mathbf{H}$,

$$\mathbf{M}(\mathbf{r},t) = \int_{-\infty}^{\infty} \chi_m(t-\tau)\mathbf{H}(\mathbf{r},\tau)\mathrm{d}\tau. \tag{6}$$

The integral in this equation, which is valid for dispersive magnetic media exhibiting cubic symmetry, again accounts for the strong dispersion typical for metamaterials. Substitution of Eqs. (1) and (6) in Maxwell's equations[53] leads to a wave equation governing the electric field $\mathbf{E}$ in a (nonlinear) left-handed material,

$$-\nabla\times\nabla\times\mathbf{E}(\mathbf{r},t) - \frac{1}{c^2}\int_{-\infty}^{\infty}\mu_r(t-\tau)\frac{\partial^2}{\partial\tau^2}\int_{-\infty}^{\infty}\epsilon_r(\tau-u) \times \mathbf{E}(\mathbf{r},u)\mathrm{d}u\mathrm{d}\tau = \mu_0\int_{-\infty}^{\infty}\mu_r(t-\tau)\frac{\partial^2}{\partial\tau^2}\mathbf{P}^{(\mathrm{NL})}(\mathbf{r},\tau)\mathrm{d}\tau, \tag{7}$$

where $\mathbf{P}^{(\mathrm{NL})}$ is the nonlinear part of the polarization field; the explicit form of this term depends on the type of nonlinearity.

Again we can apply the slowly varying envelope approximation by representing the light signal by a wave packet of the form of Eq. (3). Under the same approximations as before, a multiple scales perturbation technique can be applied to the wave equation. The additional integral representing magnetic dispersion can be treated in the frequency domain as a frequency-dependent permeability. When special care is taken to include this dispersive magnetic effect, the perturbation analysis leads to a new nonlinear Schrödinger equation for the propagation of light in a left-handed material with a Kerr nonlinearity,

$$\frac{\partial A}{\partial \xi} = \frac{ic}{2\omega n}\nabla_\perp^2 A - \frac{i\beta}{2}\frac{\partial^2 A}{\partial t^2} + \frac{i3\omega}{2c\eta}\chi^{(3)}|A|^2 A. \tag{8}$$

This equation has the same form as Eq. (5), but differs by its coefficients. First, we see that an additional parameter, the characteristic impedance η, shows up to complement the index of refraction. It can be shown that η remains positive for left-handed materials, whereas the index of refraction becomes negative.[34] This also implies that the sign of the nonlinear term does not change in left-handed materials, but that the coefficient in front of the diffraction term becomes *negative* in such a material.

In some systems, different waves will interact through the nonlinear polarization term. This occurs, for example, in Fabry-Perot resonators, where both forward and backward waves are important. Technically, this coupling between different linear modes will arise as additional terms in the perturbation analysis mentioned above, leading to the following coupled nonlinear Schrödinger equations:

$$\frac{\partial A_f}{\partial \xi} = \frac{ic}{2\omega n}\nabla_\perp^2 A_f - \frac{i\beta}{2}\frac{\partial^2 A_f}{\partial t^2} + \frac{i3\omega}{2c\eta}\chi(|A_f|^2 + 2|A_b|^2)A_f, \tag{9}$$

$$\frac{\partial A_b}{\partial \zeta} = -\frac{ic}{2\omega n}\nabla_\perp^2 A_b + \frac{i\beta}{2}\frac{\partial^2 A_b}{\partial t^2} - \frac{i3\omega}{2c\eta}\chi(|A_b|^2 + 2|A_f|^2)A_b, \tag{10}$$

where ξ and ζ are the coordinates of reference frames moving with group velocity in forward and backward directions, respectively.

Nonlinear coupling occurs also in systems with a second-order nonlinearity, where two waves of different frequencies are coupled: a pump wave A_p at center frequency ω, and a signal wave A_s at frequency $\omega/2$. For such systems, the appropriate propagation equations become

$$\frac{\partial A_s}{\partial z} + \frac{n_s}{c}\frac{\partial A_s}{\partial t} = \frac{i\omega\chi^{(2)}}{c\eta_s}A_p A_s^* + \frac{ic}{2\omega n_s}\nabla_\perp^2 A_s - \frac{i\beta}{2}\frac{\partial^2 A_s}{\partial t^2}, \tag{11}$$

$$\frac{\partial A_p}{\partial z} + \frac{n_p}{c}\frac{\partial A_p}{\partial t} = \frac{i\omega\chi^{(2)}}{2c\eta_p}A_s^2 + \frac{ic}{\omega n_p}\nabla_\perp^2 A_p - \frac{i\beta}{2}\frac{\partial^2 A_p}{\partial t^2}. \tag{12}$$

Again, the negative refractive index of a left-handed material will reverse the sign of the diffraction coefficient. Here we should note that the existing metamaterials can have a negative index of refraction at either signal or pump frequency.

III. MEAN-FIELD MODELS FOR RESONATORS WITH LEFT-HANDED MATERIALS

The propagation equations derived in the preceding section can be generally used to model the spatiotemporal dynamics of nonlinear optical resonators, such as dispersive Kerr resonators [see Fig. 1(a)] and degenerate optical parametric oscillators [see Fig. 1(b)]. Every material layer can be described by a separate nonlinear Schrödinger equation, and appropriate boundary conditions must be added to describe the interfaces between the layers. Nevertheless, if one is only interested in the dynamics of the emitted field, and not in the longitudinal evolution of the radiation inside the cavity, it is useful to simplify the set of propagation models to equations only involving the input and output amplitudes. This is possible when the field intensity does not vary appreciably over one round trip. For traditional Kerr resonators, this is achieved by the so-called Lugiato-Lefever equation.[54] The

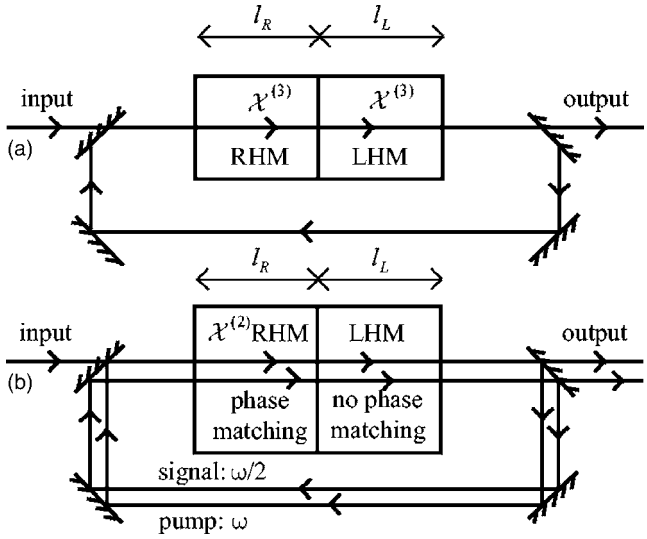

FIG. 1. Nonlinear optical systems containing a left-handed material that are studied in this paper. (a) A dispersive Kerr resonator with two layers of material: one layer consists of a right-handed medium, the other layer consists of a left-handed material. (b) A degenerate optical parametric oscillator with a left-handed material in a ring cavity. Pump and signal field are coupled by the $\chi^{(2)}$ crystal.

validity of the mean-field approximations leading to such equations has been verified in Ref. 55. Mean-field equations have been derived for Kerr cavities containing left-handed materials in Ref. 56. We recall the main steps of this derivation and we extend the results to $\chi^{(2)}$ media. Here, we will greatly simplify the mathematics by assuming that no backward field propagates in the cavity, and that the system is stationary with respect to the fast time t. These assumptions were shown to be valid in Ref. 56.

In the case of a $\chi^{(3)}$ medium, the optical propagation is described by Eq. (8), where we set $\beta=0$ since we do not consider dispersion effects here. The boundary conditions in the cavity correspond to the set of equations

$$A_C(-l_R) = t_{\text{in}}A_{\text{in}} + r_{\text{in}}r_{\text{out}}e^{i\varphi}A_C(l_L), \tag{13}$$

$$A_R(-l_R) = t_R A_C(-l_R), \tag{14}$$

$$A_L(0) = A_R(0), \tag{15}$$

$$A_C(l_L) = t_L A_L(l_L), \tag{16}$$

where the subscripts denote the medium in which the field is considered, i.e., R and L for the right-handed and left-handed materials, and C for the cavity. The interface between the right-handed and left-handed material is taken to be the origin of the longitudinal coordinate. The letters "t" and "r" denote the transmission and the reflection coefficients, l_R and l_L are the lengths of the material layers as indicated in Fig. 1, φ is the linear phase accumulated by the wave during one round trip, and A_{in} is the pump field. The two lower mirrors in Fig. 1 can be considered to be perfectly reflecting. The boundary conditions can be simplified in the form

$$A_R(-l_R) = t_R t_{\text{in}}A_{\text{in}} + t_R r_{\text{in}}r_{\text{out}}e^{i\varphi}t_L A_L(l_L), \tag{17}$$

$$A_L(0) = A_R(0). \tag{18}$$

It is important to note that Eq. (18) means that there are no reflections at the interface between the right-handed and left-handed materials. This requires that both materials are impedance matched, which is possible since the impedance of a left-handed material can be tuned independently from its index of refraction. In another possible realization, an optical isolator could be used to inhibit the counterpropagating wave that would appear due to this reflection.

Combining these conditions with the first-order expansion of the propagation equations in the right-handed and the left-handed materials [Eq. (9)] leads to

$$\begin{aligned} A_C^{(n)}(-l_R) = {} & t_{\text{in}}A_{\text{in}} + r_{\text{in}}r_{\text{out}}t_L t_R e^{i\varphi}[1 + il_L\gamma_L|A_L(0)|^2] \\ & \times\left(1 + i\frac{l_L}{k_L}\nabla_\perp^2\right)\left(1 + i\frac{l_R}{k_R}\nabla_\perp^2\right) \\ & \times[1 + il_R\gamma_R|A_R(-l_R)|^2]A^{(n-1)}(-l_R), \end{aligned} \tag{19}$$

where $A_C^{(n)}$ is the envelope of the field after n round trips in the cavity. In what follows, we will only keep the terms in Eq. (19) that are linear in l_L and l_R. This is allowed since we adopt the mean-field approximations, which state that the round-trip length of the cavity is smaller than the typical lengths over which diffraction and nonlinear effects take place.

In the frame of the mean-field approximation, the intensity variation of the field in one material slice is negligible, so that $|A_L(0)|^2=|A_R(-l_R)|^2=t_R^2|A_C(-l_R)|^2$. These last identities and the definition of the slow time τ together with that of the round-trip time T_r allow us to replace the infinite map given by Eq. (19) by a single partial differential equation,

$$A^{(n)} - A^{(n-1)} \approx T_r \left.\frac{\partial A}{\partial \tau}\right|_{\tau=nT_r}. \tag{20}$$

This equation can be further simplified if we assume that the resonance condition in the cavity is almost fulfilled ($r_{\text{in}}r_{\text{out}}t_L t_R e^{i\varphi} \approx |r_{\text{in}}r_{\text{out}}t_L t_R|$). In what follows, we can therefore introduce $\rho=|r_{\text{in}}r_{\text{out}}t_L t_R|$ and the detuning between the pump field and the cavity mode $\theta \ll 1$, so that $r_{\text{in}}r_{\text{out}}t_L t_R e^{i\varphi} = \rho e^{i\theta} \approx \rho(1+i\theta)$.

The equation describing the evolution of the amplitude of the electric field in the cavity is therefore

$$\begin{aligned} T_r\frac{\partial A}{\partial \tau} = {} & t_{\text{in}}A_{\text{in}} - (1-\rho)A + \rho\left(\frac{l_L}{k_L} + \frac{l_R}{k_R}\right)\nabla_\perp^2 A + i\rho\theta A \\ & + i\rho(l_L\gamma_L + l_R\gamma_R)t_R^2|A|^2 A. \end{aligned} \tag{21}$$

Finally, we write this equation in a nondimensionalized form,[54]

$$\frac{\partial A}{\partial T} = -(1 + i\Delta)A + \mathcal{E} + i\Gamma|A|^2 A + i\mathcal{D}\nabla_\perp^2 A, \tag{22}$$

with $T=(1-\rho)\tau/T_r$. In this equation, Δ is the normalized cavity detuning, Γ is the normalized nonlinear Kerr coefficient, and $\mathcal{E}$ is the normalized amplitude of the input field. The diffraction coefficient $\mathcal{D}$ will be discussed later in this section.

A similar handling of the $\chi^{(2)}$ case leads to the same kind of boundary conditions, with the main difference being that we must now take into account two fields: one at the pump frequency $\omega_p=2\omega$ and the other at the signal frequency $\omega_s=\omega$. We find

$$A_{C,p}(-l_R) = t_{\mathrm{in},p}A_{\mathrm{in},p} + r_{\mathrm{in},p}r_{\mathrm{out},p}e^{i\varphi_p}A_{C,p}(l_L), \tag{23}$$

$$A_{C,s}(-l_R) = r_{\mathrm{in},s}r_{\mathrm{out},s}e^{i\varphi_s}A_{C,s}(l_L). \tag{24}$$

The equations describing the propagation are now given by Eqs. (11) and (12). Their first-order expansions

$$A_{L,p}(l_L) = A_{R,p}(-l_R) + i\left(\frac{l_R}{k_{R,p}} + \frac{l_L}{k_{L,p}}\right)A_{R,p}(-l_R) + il_R\frac{\omega_p\chi^{(2)}}{4c\eta_p}A_{C,s}^2(-l_R), \tag{25}$$

$$A_{L,s}(l_L) = A_{R,s}(-l_R) + i\left(\frac{l_R}{k_{R,s}} + \frac{l_L}{k_{L,s}}\right)A_{R,s}(-l_R) + il_R\frac{\omega_s\chi^{(2)}}{c\eta_s}A_{C,p}(-l_R)A_{C,s}^*(-l_R), \tag{26}$$

and the boundary conditions (23) and (24) lead to an infinite set of equations. As previously, we introduce the round-trip time T_r in order to replace this infinite set of equations by two partial differential equations. Assuming that we are near resonance, we find

$$T_r\frac{\partial A_p}{\tau} = t_{\mathrm{in},p}A_{\mathrm{in}} + (r_{\mathrm{in},p}r_{\mathrm{out},p}t_{L,p}e^{i\varphi_p} - 1)A_p + ir_{\mathrm{in},p}r_{\mathrm{out},p}t_{L,p}e^{i\varphi_p}\times\left[\left(\frac{l_L}{k_{L,p}} + \frac{l_R}{k_{R,p}}\right)\nabla_\perp^2 A_p + l_R\frac{\omega_p\chi^{(2)}}{4c\eta_p}A_s^2\right], \tag{27}$$

$$T_r\frac{\partial A_s}{\tau} = (r_{\mathrm{in},s}r_{\mathrm{out},s}t_{L,s}e^{i\varphi_s} - 1)A_s + ir_{\mathrm{in},s}r_{\mathrm{out},s}t_{L,s}e^{i\varphi_s}\times\left[\left(\frac{l_L}{k_{L,s}} + \frac{l_R}{k_{R,s}}\right)\nabla_\perp^2 A_s + l_R\frac{\omega_s\chi^{(2)}}{c\eta_s}A_pA_s^*\right], \tag{28}$$

or, in nondimensional form,

$$\frac{\partial A_p}{\partial T} = \mathcal{E} - (1+i\Delta_p)A_p + i\mathcal{D}_p\nabla_\perp^2 A_p + i\sigma_pA_s^2, \tag{29}$$

$$\frac{\partial A_s}{\partial T} = -(1+i\Delta_s)A_s + i\mathcal{D}_s\nabla_\perp^2 A_s + i\sigma_sA_pA_s^*. \tag{30}$$

In all mean-field equations derived above, the diffraction coefficients are proportional to

$$\mathcal{D} \propto \left(\frac{l_R}{k_R} + \frac{l_L}{k_L}\right). \tag{31}$$

Recalling that the wavenumber k_L in the left-handed material is negative, we conclude that both terms in Eq. (31) will cancel each other to some extent. By choosing the thicknesses of the layers, it is therefore possible to alter the strength of diffraction during one round trip in the cavity. If the left-handed material layer is sufficiently long, the second term will dominate, and the diffraction coefficient $\mathcal{D}$ becomes negative. It is this regime of negative diffraction that we will study in the remainder of this paper.

In the degenerate parametric oscillator, the above discussion applies to both $\mathcal{D}_p$ and $\mathcal{D}_s$, which can be controlled in strength and sign. We assume phase matching between the signal and pump field only in the quadratic crystal, and not in the left-handed material. This means that there is no fixed relation between $\mathcal{D}_s$ and $\mathcal{D}_p$.

IV. KERR RESONATORS CONTAINING LEFT-HANDED MATERIALS

In this section, we will consider the first of our two prototype devices to investigate the influence of left-handed materials in nonlinear cavity optics. The Kerr resonator is an optical resonator containing a third-order nonlinearity, for which the polarization field generates spectral components at the fundamental frequency. Therefore, the Kerr resonator can be considered as one of the easiest geometries, and it is also mathematically less demanding to handle.

The structure of this section is as follows. First, we discuss the linear stability of the homogeneous output states in Sec. IV A, which will give us information on where dissipative structures can exist. We continue with the results of our weakly nonlinear analysis and numerical study to characterize the emerging patterns (Sec. IV B).

A. Linear stability analysis

When diffraction is positive, Eq. (22) is known as the Lugiato-Lefever equation.[54] Dissipative structures due to the interplay between the Kerr nonlinearity and diffraction have been predicted in this system by several authors[21–23,54,57] and are now understood fairly well. However, when the thicknesses of the right-handed and left-handed material layers in the cavity of the Kerr resonator are tuned such that the diffraction coefficient $\mathcal{D}$ becomes negative, the spatiotemporal dynamics are altered drastically. The homogeneous steady-state solutions A_s of Eq. (22) remain unaltered and are given by the implicit formula $[1+i(\Delta-\Gamma|A_s|^2)]A_s=\mathcal{E}$. It can further be shown that the homogeneous steady-state solutions (HSS) are monostable with respect to the pump $\mathcal{E}$ for $\Delta<\sqrt{3}$, whereas they are multiple valued for $\Delta>\sqrt{3}$. The linear stability analysis of these HSS can be performed by linearizing Eq. (22) around A_s. The modes of the linearized equation consistent with the boundary conditions of an extended system are given by $\exp(i\mathbf{k}\cdot\mathbf{r}_\perp-\lambda t)$. The marginal stability condition depends on the transverse wavenumber $\mathbf{k}$ of these modes,

$$1 + (\Delta + \mathcal{D}k^2 - 2\Gamma|A_s|^2)^2 = 0. \tag{32}$$

In Fig. 2, we have plotted the marginal stability curves for several values of the detuning Δ. From these figures, it becomes clear how the stability is altered when the sign of the diffraction coefficient is changed.

For positive diffraction, $\mathcal{D}k^2$ is positive, and only the upper half plane of the graphs in Fig. 2 represents modulated

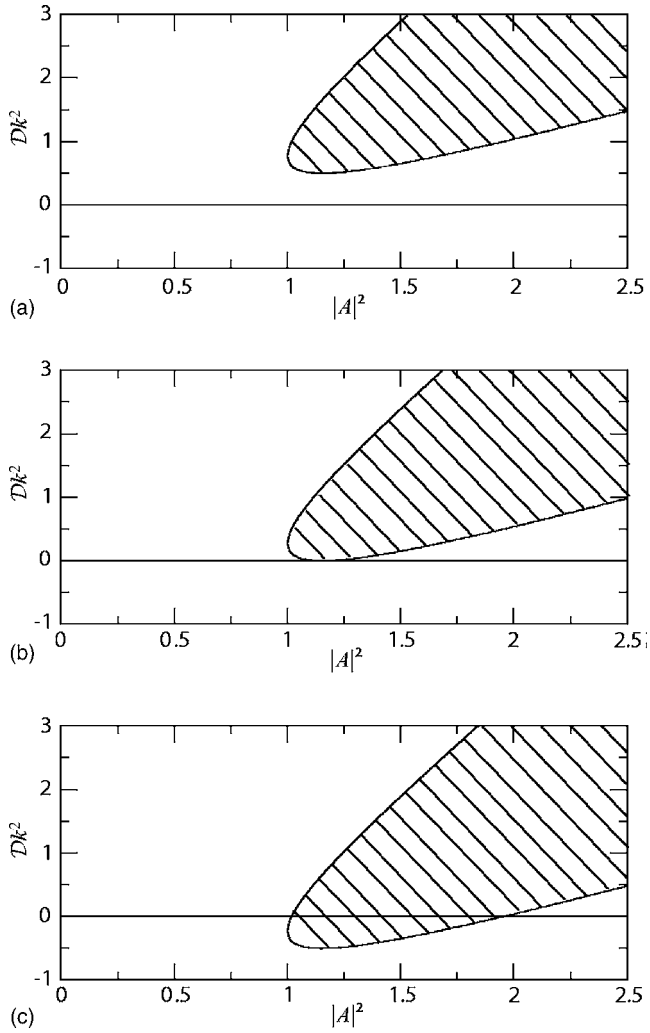

FIG. 2. Marginal stability curves for several values of the detuning parameter. The hatched region contains the unstable homogeneous states. (a) $\Delta=\sqrt{3}$. (b) $\Delta=\sqrt{3.5}$. (c) $\Delta=\sqrt{5}$.

modes. For $\Delta<2$, the homogeneous steady states with $|A|^2>1$ are destabilized by a continuum of unstable modes (hatched region in Fig. 2), and a modulational instability thus appears at $|A|^2=1$. However, when $\Delta>2$, the extremum of the marginal stability curve at $|A|^2=1$ sinks below the $\mathcal{D}k^2=0$ axis, out of the region representing modulated modes. It can be shown that in this case, the intensity where the marginal stability curve crosses the axis equals the intensity of the up-switching point, $|A_\uparrow|^2=(2\Delta-\sqrt{\Delta^2-3})/3$, and the critical point coincides with the switching point.

On the other hand, for negative diffraction ($\mathcal{D}<0$), it is the lower half plane of the graphs that denotes modulated modes. We immediately observe that all homogeneous states with an intensity higher than that where the marginal stability curve crosses the axis for the second time are stable. Since this is the intensity of the down-switching point, $|A_\downarrow|^2=(2\Delta+\sqrt{\Delta^2-3})/3$, we can conclude that the upper branch is completely stabilized by the negative diffraction. For $\Delta<2$, only the states with an intensity between the switching points $|A_\uparrow|^2$ and $|A_\downarrow|^2$ are unstable. This means that for such values of the detuning, only the negative slope branch of the bistability curve is modulationally unstable.

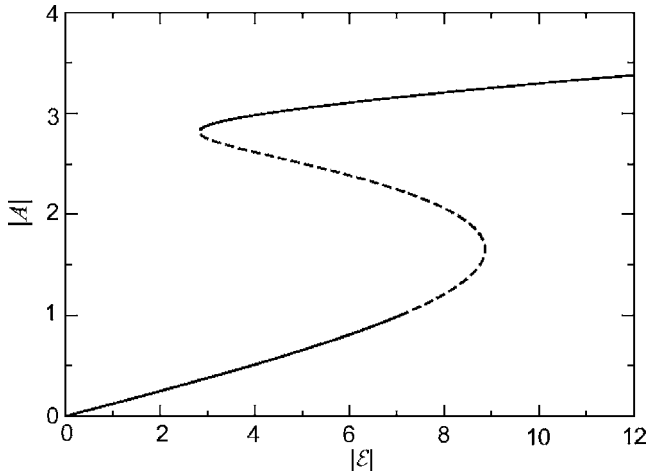

FIG. 3. Bistability curve relating the intensity of the input and output waves for $\Delta=8$ when diffraction is negative. Full lines indicate stable homogeneous states; dashed lines indicate modulationally unstable states. Note the coexistence of stable states on the upper branch and unstable states on the lower branch.

For $\Delta>2$, the extremum of the marginal stability curve at $|A|^2=1$ again sinks below the $\mathcal{D}k^2=0$ axis, but now into the allowed region. This results in a modulational instability on the lower branch of the bistability curve at $|A_c|^2=1$ (see Fig. 3).

From the above discussion, we can conclude the following important points for the negative diffraction regimes: (i) The monostable regime becomes completely modulationally stable. (ii) The states on the upper branch in the bistable regime are stabilized. (iii) A new modulational instability occurs on the lower branch of the bistability curve for $\Delta>2$ (see Fig. 3).

B. Weakly nonlinear and numerical analysis

The linear stability analysis shows that a portion of the lower homogeneous steady-state branch becomes unstable with respect to finite wavenumber perturbations. In this subsection, we shall describe the nonlinear evolution of the system in the vicinity of the modulational instability point $\mathcal{E}_c$. To this end, we use a weakly nonlinear theory. We assume that the system has a large aspect ration, i.e., large Fresnel number. In this case, the distance between the nearest eigenvalues is small, leading to a quasicontinuous spectrum of the Laplace operator. Next, we introduce a small parameter $\epsilon\ll 1$, which measures the distance from the critical modulational instability point: $\mathcal{E}=\mathcal{E}_c+\gamma\epsilon^2+\cdots$ We expand the intracavity field $\mathbf{X}=(\mathrm{Re}(A),\mathrm{Im}(A))^T$ and the homogeneous steady states $\bar{\mathbf{X}}$ around their critical values at the bifurcation point,

$$\mathbf{X}(\mathbf{r}_\perp,t)=\sum_{n=0}^{\infty}\epsilon^n\mathbf{X}^{(n)}(\mathbf{r}_\perp,t), \tag{33}$$

$$\bar{\mathbf{X}}(\mathbf{r}_\perp,t)=\sum_{n=0}^{\infty}\epsilon^n\bar{\mathbf{X}}^{(n)}(\mathbf{r}_\perp,t), \tag{34}$$

and we also introduce a slow time $\tau=\epsilon^2 t$. Substitution of all these expansions in the mean-field equation leads to a series

of linear problems. The solution to leading order in ϵ is given by a linear superposition of the corresponding critical modes. For systems with one transverse dimension, we find the following eigenmodes for the linearized problem:

$$A = e(\tau)\left(1 + i\frac{2-\Delta}{\Delta}\right)(e^{i\mathbf{k}\cdot\mathbf{r}} + e^{-i\mathbf{k}\cdot\mathbf{r}}), \tag{35}$$

where $e(\tau)$ is an amplitude that depends on the slow time scales. At higher orders, it becomes impossible to invert the linear system at $k=k_c$, and source terms with other wave vectors appear. To ensure that the expansion in Eq. (33) remains uniformly bounded, one must apply the Fredholm alternative, which requires that the projection of the source terms on the null space of the adjoint of the linear operator vanishes.[58] When the resulting solvability conditions are applied to the higher-order inhomogeneous problems, we find the following order-parameter equation governing the yet undetermined amplitude $e(\tau)$:

$$\frac{\partial e}{\partial t} = \alpha(\mathcal{E} - \mathcal{E}_c)e + \beta|e|^2 e, \tag{36}$$

where α and β are given by

$$\alpha = \frac{2\sqrt{1+(1-\Delta)^2}}{\Delta^2}, \tag{37}$$

$$\beta = \frac{4(30\Delta - 41)[1+(\Delta-1)^2]}{9[-1+(\Delta-1)^2]^2}. \tag{38}$$

Equation (36) has two solutions: $e=0$, which corresponds to the homogeneous solution, and $e=\pm\sqrt{-\alpha(\mathcal{E}-\mathcal{E}_c)/\beta}$, which determines the maximum and the minimum of the one-dimensional periodic dissipative structure. When $\Delta<\Delta_{\mathrm{sub}}=41/30$, the modulational instability is supercritical. The transition from a supercritical to a subcritical modulational instability occurs at $\Delta=\Delta_{\mathrm{sub}}$. This transition requires $\Delta<\sqrt{3}$, which is far from the onset of bistability. Note, however, that in the parameter range of our interest, i.e., $\Delta>2$, the modulational instability always appears subcritical. In that case, the saturation parameter $\beta>0$, and it is necessary to retain the next order in ϵ since the above amplitude equation cannot describe stable periodic structures.

In order to further characterize the emerging patterns, we have solved the mean-field equation numerically. The input is chosen in the unstable region of the lower branch of the bistability curve. We have discretized Eq. (22) with a Crank-Nicholson scheme on a 256–point grid, and we have applied periodic boundary conditions. The initial condition was taken to be the low-intensity homogeneous steady state corresponding to the given input, and a small noise term was added to this state in order to excite the unstable modes. For the Kerr resonator with one transverse dimension, we have indeed found stable stripe patterns (see Fig. 4).

An important difference appears when considering two transverse dimensions. At the threshold associated with modulational instability, the homogeneous steady-state solutions become unstable with respect to transverse wave vectors, which have all the same modulus $k=k_c$, but have no preferred direction, because the system is arbitrarily directed

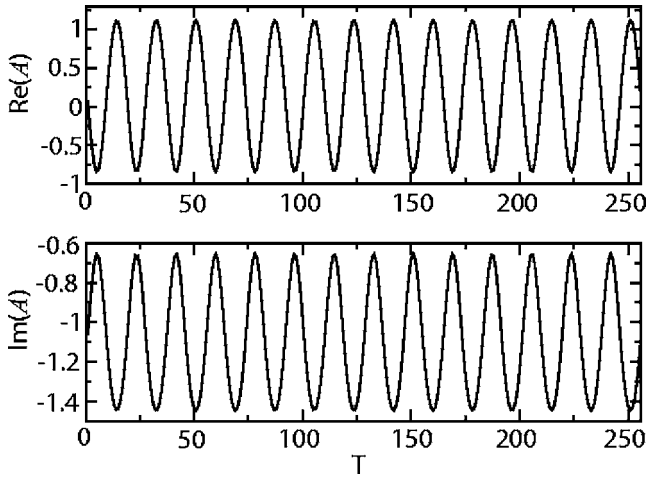

FIG. 4. Stable one-dimensional dissipative structure in the Kerr resonator with negative diffraction. Parameters are $\mathcal{D}=-5$, $\Delta=12$, and $\mathcal{E}=11$.

in the isotropic (x,y) plane. Although an indefinite number of modes are generated with arbitrary direction due to the rotational degeneracy, a regular pattern is selected and emerges due to the nonlinear interaction.

We have performed similar simulations for systems with two dimensions, and we find that these simulations yield completely different results (see Fig. 5). In systems with two transverse dimensions, we observe that the emitted field first evolves to a transient dissipative pattern with hexagonal symmetry, after which a nucleation process takes place. The pixels in the pattern merge, and the output field finally approaches the high-intensity homogeneous state. This seems to contradict the nonlinear stability analysis, but one should recall that the high-intensity homogeneous state is stabilized by the negative diffraction for every input in the region between the threshold for modulational instability and the normal switching point. This means that two spatiotemporal processes can be identified in the Kerr resonator with negative diffraction. One process is the interaction between the unstable Fourier modes, which tends to impose periodicity in the transverse space, favoring the formation of dissipative structures. The other is the restoration of uniformity in the transverse space by the stable homogeneous state. A perturbation analysis as presented in the beginning of this subsection cannot account for the second process since the stable high-intensity state is far from the threshold of modulational instability. Only our numerical analysis can reveal that the switching front dominates the spatiotemporal dynamics over the formation of dissipative structures. In Ref. 59, we have studied systems in which dispersion cannot be neglected, leading to three-dimensional structures. There, we have shown that such systems exhibit a similar behavior as described for two-dimensional systems above.

For the one-dimensional system, we can conclude that stripe patterns appear subcritically. This indicates that also localized structures—connecting the stable stripes with the homogeneous background—could exist, at least in the system with one transverse dimension. Further numerical simulations need to be performed to find such structures. An interesting feature of the negative diffraction resonator is that

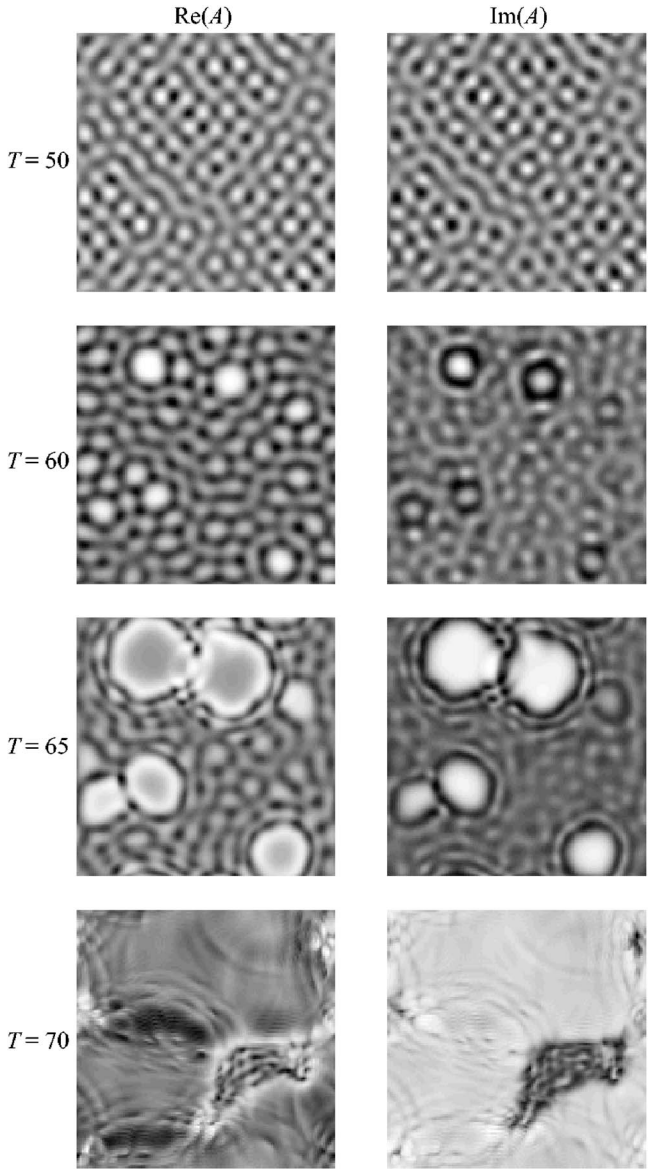

FIG. 5. Evolution of the two-dimensional emitted field. A dissipative structure seems to be formed at first, but the field finally evolves toward the stable high-intensity homogeneous state. Parameters are $\mathcal{D}=-1$, $\Delta=12$, and $\mathcal{E}=12$. The first and second rows contain plots of the real and imaginary parts of A, respectively.

the stable stripes also coexist with the *stable* high-intensity homogeneous solution, suggesting the existence of so-called dark cavity solitons. For systems with two transverse dimensions, the existence of localized structures remains to be investigated. Another interesting issue of the diffraction-managed resonator is how the geometry and size of these localized structures depend on the diffraction coefficients. This problem has been taken up recently for the positive diffraction regime.[60]

V. DEGENERATE OPTICAL PARAMETRIC OSCILLATORS CONTAINING LEFT-HANDED MATERIAL

Another prototype device based on an optical ring cavity is the degenerate optical parametric oscillator, which contains a crystal with a second-order nonlinearity to convert the energy of a pump beam at frequency ω to a signal beam at frequency $\omega/2$. The fact that there are two coupled waves in this system makes this problem mathematically more demanding. Pattern formation in optical systems with a second-order nonlinearity has been studied by several authors.[27,61–70]

In Sec. III, we have shown that the method of diffraction control by insertion of a left-handed material in a cavity can be generalized to degenerate optical parametric oscillators. This implies that our setup makes it possible to change the value and sign of the diffraction coefficients of the signal and field waves. Note also that the absence of phase matching in the left-handed material layer means that there is no fixed relationship between the diffraction coefficients $\mathcal{D}_s$ and $\mathcal{D}_p$.

A. Linear stability analysis

One can easily see that the diffraction terms in Eqs. (29) and (30) do not influence the homogeneous steady states, which are still given by the expressions reported in the literature, i.e.,

$$A_s = 0, \quad A_p = \frac{\mathcal{E}}{1 + i\Delta_p} \tag{39}$$

for the nonlasing solution, and

$$A_s = \pm e^{i\phi}\sqrt{-1 + \Delta_s\Delta_p + \sqrt{|\mathcal{E}|^2 - (\Delta_s + \Delta_p)^2}}, \tag{40}$$

$$A_p = e^{i\theta}\sqrt{1 + \Delta_1^2}, \tag{41}$$

$$\phi = -\frac{1}{2}\mathrm{atan}\left(\frac{\Delta_s + \Delta_p}{\mathcal{E}^2 - (\Delta_s + \Delta_p)}\right), \tag{42}$$

$$e^{i\theta} = \frac{1 + i\Delta_s}{\sqrt{1 + \Delta_s^2}}e^{i2\phi} \tag{43}$$

for the lasing solution. Without diffraction, the nonlasing solution is stable for input amplitudes $\mathcal{E}<\mathcal{E}_T$, with

$$\mathcal{E}_T = \sqrt{1 + \Delta_p^2}\sqrt{1 + \Delta_s^2}. \tag{44}$$

At the lasing threshold $\mathcal{E}_T$, a first bifurcation occurs: the nonlasing solution becomes unstable, and the lasing solutions appear. Here, we investigate the formation of dissipative structures for inputs below the lasing threshold $\mathcal{E}_T$, i.e., structures emerging from the nonlasing solution. We have performed a linear stability analysis of the nonlasing states, carefully allowing for negative values of the diffraction coefficients. We find the following marginal stability condition depending on the wavenumber $\mathbf{k}$ of the Fourier modes $\exp(i\mathbf{k}\cdot\mathbf{r}_\perp - \lambda t)$:

$$\mathcal{E} = \sqrt{1 + \Delta_p^2}\sqrt{1 + (\Delta_s + \mathcal{D}_s k^2)^2}. \tag{45}$$

From this condition, we see that the smallest value of $\mathcal{E}$ where the homogeneous solution becomes modulationally unstable is given by $\mathcal{E}_M = \sqrt{1+\Delta_p^2}$. All homogeneous solutions in the input range $\mathcal{E}_M<\mathcal{E}<\mathcal{E}_T$ are unstable with respect to modulated modes. At the onset of modulational instability ($\mathcal{E}=\mathcal{E}_M$), only the modes that have their wavenumber given by $\mathcal{D}_s k_c^2 = -\Delta_s$ are unstable, resulting in the formation of dissipative structures with wavelength

$$\Lambda = 2\pi\sqrt{-\frac{\mathcal{D}_s}{\Delta_s}}. \tag{46}$$

Note that negative diffraction of the signal field allows for dissipative structures in cavities with positive detuning $\Delta_s > 0$.

B. Weakly nonlinear analysis

Similarly to the analysis for the Kerr resonator, we can make a perturbation expansion around the threshold of modulational instability. Following the procedure outlined in Ref. 61, we expand the fields $\mathbf{X} = (\mathrm{Re}(A_p), \mathrm{Im}(A_p), \mathrm{Re}(A_s), \mathrm{Im}(A_s))^T$ in a Taylor expansion of ϵ,

$$\mathbf{X}(\mathbf{r}_\perp, t) = \sum_{n=0}^{\infty} \epsilon^n \mathbf{X}^{(n)}(\mathbf{r}_\perp, t), \tag{47}$$

where $\epsilon = (\mathcal{E} - \mathcal{E}_M)/\mathcal{E}_M$ is a smallness parameter related to the distance from the threshold. Substitution of Eq. (47) and the homogeneous states given by Eq. (39) in Eqs. (29) and (30) leads to a series of linear problems. The first-order solution gives only a contribution to the signal field,

$$A_s = [\Delta_p + i(1 - \sqrt{1 + \Delta_p^2})]e(T_1, T_2, \ldots) \times (e^{i\mathbf{k}_c \cdot \mathbf{r}} + e^{-i\mathbf{k}_c \cdot \mathbf{r}}), \tag{48}$$

where we have again included only two critical modes in order to describe one-dimensional systems or stripe patterns in systems with more transverse dimensions. The solvability condition of the second-order problem then yields a correction to the homogeneous pump field generated due to the nonlinear mixing of the signal field,

$$A_p = e^2(T_1, T_2, \ldots)[2a + be^{i2\mathbf{k}_c \cdot \mathbf{r}} + be^{-i2\mathbf{k}_c \cdot \mathbf{r}}], \tag{49}$$

with a and b constants depending only on the geometry of the cavity,

$$a = \frac{-2(\Delta_p + i)^2(1 - \sqrt{1 + \Delta_p^2})}{1 + \Delta_p^2}, \tag{50}$$

$$b = \frac{-2(\Delta_p + i)(\Delta_p + 4\mathcal{D}_p k_c^2 + i)(1 - \sqrt{1 + \Delta_p^2})}{1 + (\Delta_p + 4\mathcal{D}_p k_c^2)^2}. \tag{51}$$

The undetermined slowly varying amplitude e can finally be fixed from the solvability condition at third order. We find the following order-parameter equation for the dynamics of $e(T_1, T_2, \ldots)$:

$$\frac{\partial e}{\partial t} = \alpha(\mathcal{E} - \mathcal{E}_c)e - \beta|e|^2 e, \tag{52}$$

where α and β are positive numbers given by

$$\alpha = 1, \tag{53}$$

$$\beta = \left(2\mathcal{D}_p k_c^2 + \frac{3\Delta}{4}\right)\mathrm{Re}(b) - \frac{3}{4}\,\mathrm{Im}(b). \tag{54}$$

Again, we find two stationary solutions to Eq. (36): $e = 0$, corresponding to the homogeneous solution, and $e = \sqrt{\alpha(\mathcal{E} - \mathcal{E}_c)/\beta}$, corresponding to stripes. However, for the DOPO, we see that the stripes branch always appears supercritically. We can therefore immediately conclude that stable dissipative structures must exist in the vicinity of the threshold of modulational instability.

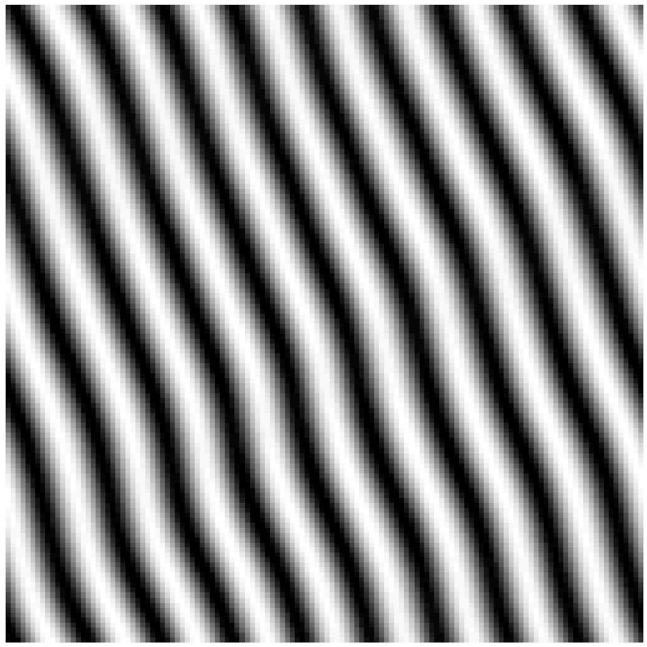

FIG. 6. Stripes pattern in the degenerate optical parametric oscillator with negative diffraction and positive detuning. Parameters are $\Delta_s = \Delta_p = 2.0$, $\mathcal{E} = 2.5$, and $\mathcal{D}_s = \mathcal{D}_p = -1.5$.

C. Numerical analysis

Finally, we verify the prediction from the weakly nonlinear analysis with a simulation. We have discretized Eqs. (29) and (30) with a Crank-Nicholson scheme on a 128×128 grid, applying periodic boundary conditions. The initial condition consists of the homogeneous state to which a small noise term is added in order to excite the unstable modes. In Fig. 6, we show stripe patterns obtained from simulations. When diffraction is negative, we have indeed found stripes as predicted by our analytical analysis. We observe both regular stripes and labyrinthic rolls depending on the intensity of the input beam. The wavelength of these patterns is in agreement with the value predicted by the linear stability analysis. The negative diffraction due to the left-handed material thus allows for dissipative patterns in a degenerate optical parametric oscillator with positive detunings, whereas in the classical resonator with positive diffraction, such structures only emerge when the detuning of the signal wave is negative. The influence of the ratio of the diffraction coefficients, $\mathcal{D}_s/\mathcal{D}_p$, requires further investigation.

VI. CONCLUSIONS AND OUTLOOK

In this paper, we have investigated pattern formation in nonlinear resonators containing a left-handed material. We have shown quite generally that the insertion of a left-handed material in an optical cavity allows for control on its diffrac-

tion properties: it is not only possible to change the strength of diffraction, but also to tune the system in a regime of negative diffraction. We have further studied pattern formation in two prototype systems of nonlinear optics based on an optical resonator: a dispersive Kerr resonator and a degenerate optical parametric oscillator. For the Kerr resonator, we have shown that stable stripes only exist in systems with one transverse dimension. In systems with more transverse dimensions, the formation of dissipative structures induces a switching process toward the high-intensity homogeneous state. For the degenerate optical oscillator, we have shown the existence of stable two-dimensional structures in systems with positive detunings, which is not possible in traditional degenerate optical parametric oscillators.

The existence of extended dissipative structures in the systems under study indicates that also localized structures may be found. In the one-dimensional Kerr resonator, where a stable stripe pattern coexists with the homogeneous state, one expects a localized structure connecting both solutions. Furthermore, other types of localized structures, e.g., connecting the stable high-intensity background to the stripes, could also exist. We intend to study these issues related to the formation of such localized structures. In systems with more transverse dimensions, the existence of localized solutions needs to be investigated with numerical simulations. If the switching process indeed always dominates the spatiotemporal dynamics, then we have a system with two nonsymmetric coexisting stable homogeneous states, for which we intend to study the front dynamics. For the degenerate optical parametric oscillator, we will explore the spatiotemporal dynamics above the lasing threshold. The control of the strength and sign of diffraction may also drastically alter the geometric properties and the size of these localized structures. We therefore intend to study the relation between the diffraction coefficients and the size of localized structures.

ACKNOWLEDGMENTS

P. T. and L.G. are Ph.D. Fellows and G.V. is a Postdoctoral Fellow of the Research Foundation-Flanders (FWO-Vlaanderen). M.T. is a Research Associate of the Fonds National de la Recherche Scientifique (FNRS). This work was financially supported by the Belgian Science Policy Office under Grant No. IAP P6/10 and by the Research Council (OZR) of the Vrije Universiteit Brussel.

[1] A. M. Turing, Philos. Trans. R. Soc. London, Ser. B **237**, 37 (1952).
[2] P. Glansdorff and I. Prigogine, *Thermodynamic Theory of Structures, Stability and Fluctuations* (Wiley, New York, 1971).
[3] E. Meron, Phys. Rep. **218**, 1 (1992).
[4] M. C. Cross and P. C. Hohenberg, Rev. Mod. Phys. **65**, 851 (1992).
[5] J. D. Murray, *Mathematical Biology* (Springer, Berlin, 1993).
[6] B. S. Kerner and V. V. Osipov, *Autosolutions, a New Approach to Problems of Self-Organization and Turbulence* (Kluwer, Dordrecht, 1994).
[7] J. Chanu and R. Lefever, Physica A **213**, 1 (1995).
[8] K. Kapral and K. Showalter, *Chemical Waves and Patterns* (Kluwer, Dordrecht, 1995).
[9] L. A. Lugiato, M. Brambilla, and A. Gatti, *Optical Pattern Formation*, Vol. 40 of Advances in Atomic, Molecular and Optical Physics (Academic Press, New York, 1998).
[10] F. T. Arecchi, S. Boccaletti, and P. L. Ramazza, Phys. Rep. **318**, 1 (1999).
[11] W. Lange and T. Ackemann, J. Opt. B: Quantum Semiclassical Opt. **2**, 347 (2000).
[12] M. I. Rabinovich and A. B. Ezersky, *The Dynamics of Patterns* (World Scientific, Singapore, 2000).
[13] N. N. Rosanov, *Spatial Hysteresis and Optical Patterns*, Springer Series in Synergetics (Springer, Berlin, 2002).
[14] K. Staliunas and V. J. Sanchez-Morcillo, *Transverse Patterns in Nonlinear Optical Resonators*, Vol. 183 of Springer Tracts in Modern Physics (Springer-Verlag, Berlin, 2003).
[15] L. A. Lugiato, IEEE J. Quantum Electron. **39**, 193 (2003).
[16] P. Mandel and M. Tlidi, J. Opt. B: Quantum Semiclassical Opt. **6**, 60 (2004).
[17] C. Denz, M. Schwab, and C. Weilnau, *Transverse Pattern Formation in Photorefractive Optics*, Vol. 188 of Springer Tracts in Modern Physics (Springer, Berlin, 2005).
[18] R. Hoyle, *Pattern Formation: An Introduction to Methods* (Cambridge University Press, Cambridge, UK, 2006).
[19] B. A. Malomed, *Soliton Management in Periodic Systems* (Springer, New York, 2006).
[20] M. Tlidi, P. Mandel, and R. Lefever, Phys. Rev. Lett. **73**, 640 (1994).
[21] A. J. Scroggie, W. J. Firth, G. S. McDonald, M. Tlidi, R. Lefever, and L. A. Lugiato, Chaos, Solitons Fractals **4**, 1323 (1994).
[22] D. Gomila, M. A. Matías, and P. Colet, Phys. Rev. Lett. **94**, 063905 (2005).
[23] D. Gomila, A. Jacobo, M. A. Matías, and P. Colet, Phys. Rev. E **75**, 026217 (2007).
[24] S. Longhi, Opt. Lett. **23**, 346 (1998).
[25] C. Etrich, U. Peschel, and F. Lederer, Phys. Rev. Lett. **79**, 2454 (1997).
[26] K. Staliunas and V. J. Sanchez-Morcillo, Opt. Commun. **139**, 306 (1997).
[27] P. Lodahl and M. Saffman, Opt. Commun. **184**, 493 (2000).
[28] S. Barland, J. R. Tredicce, M. Brambilla *et al.*, Nature (London) **419**, 699 (2002).
[29] A. Barsella, C. Lepers, and M. Taki, Opt. Commun. **181**, 401 (2000).
[30] V. B. Taranenko, K. Staliunas, and C. O. Weiss, Phys. Rev. A **56**, 1582 (1997).
[31] M. Tlidi, P. Mandel, and M. Haelterman, Phys. Rev. E **56**, 6524 (1997).
[32] M. Pesch, E. Große Westhoff, T. Ackemann, and W. Lange, Phys. Rev. Lett. **95**, 143906 (2005).
[33] L. I. Mandelstam, Zh. Eksp. Teor. Fiz. **15**, 475 (1945).
[34] V. G. Veselago, Sov. Phys. Usp. **10**, 509 (1968).
[35] R. A. Shelby, D. R. Smith, and S. Schultz, Science **292**, 77 (2001).
[36] J. B. Pendry, A. J. Holden, D. J. Robbins, and W. J. Stewart, IEEE Trans. Microwave Theory Tech. **47**, 2075 (1999).
[37] D. R. Smith, W. J. Padilla, D. C. Vier, S. C. Nemat-Nasser, and S. Schultz, Phys. Rev. Lett. **84**, 4184 (2000).
[38] S. Zhang, W. Fan, K. J. Malloy, S. R. J. Brueck, N. C. Panoiu, and R. M. Osgood, J. Opt. Soc. Am. B **23**, 434 (2006).
[39] G. Dolling, C. Enkrich, M. Wegener, C. M. Soukoulis, and S. Linden, Opt. Lett. **31**, 1800 (2006).
[40] V. M. Shalaev, Nat. Photonics **1**, 41 (2007).
[41] J. B. Pendry, D. Shurig, and D. R. Smith, Science **312**, 1780 (2006).
[42] U. Leonhardt, Science **312**, 1777 (2006).
[43] J. B. Pendry, Phys. Rev. Lett. **85**, 3966 (2000).
[44] D. Schurig and D. R. Smith, Phys. Rev. E **70**, 065601 (2004).
[45] P. Tassin, I. Veretennicoff, and G. Van der Sande, Opt. Commun. **264**, 130 (2006).
[46] A. A. Zharov, I. V. Shadrivov, and Y. S. Kivshar, Phys. Rev. Lett. **91**, 037401 (2003).
[47] N. Lazarides and G. P. Tsironis, Phys. Rev. E **71**, 036614 (2005).
[48] G. D'Aguanno, N. Mattiucci, M. Scalora, and M. J. Bloemer, Phys. Rev. Lett. **93**, 213902 (2004).
[49] A. A. Zharov, N. A. Zharova, I. V. Shadrivov, and Y. S. Kivshar, Appl. Phys. Lett. **87**, 091104 (2005).
[50] I. V. Shadrivov, A. A. Zharov, and Y. S. Kivshar, J. Opt. Soc. Am. B **23**, 529 (2006).
[51] J. V. Moloney and A. C. Newell, *Nonlinear Optics* (Westview Press, Boulder, CO, 2003).
[52] M. Scalora, M. S. Syrchin, N. Akozbek, E. Y. Poliakov, G. D'Aguanno, N. Mattiucci, M. J. Bloemer, and A. M. Zheltikov, Phys. Rev. Lett. **95**, 013902 (2005).
[53] J. D. Jackson, *Classical Electrodynamics* (Wiley, New York, 1999).
[54] L. A. Lugiato and R. Lefever, Phys. Rev. Lett. **58**, 2209 (1987).
[55] M. Tlidi, M. Le Berre, E. Ressayre, and A. Tallet, Phys. Rev. A **61**, 043806 (2000).
[56] P. Kockaert, P. Tassin, G. Van der Sande, I. Veretennicoff, and M. Tlidi, Phys. Rev. A **74**, 033822 (2006).
[57] G. Grynberg, Opt. Commun. **66**, 321 (1988).

[58]I. Stakgold, *Green's Functions and Boundary Value Problems*, 2nd ed. (Wiley, New York, 1998).
[59]P. Tassin, G. Van der Sande, N. Veretenov, P. Kockaert, I. Veretennicoff, and M. Tlidi, Opt. Express **14**, 9338 (2006).
[60]L. Gelens, G. Van der Sande, G. Tassin, M. Tlidi, P. Kockaert, D. Gomila, I. Veretennicoff, and J. Danckaert, Phys. Rev. A **75**, 063812 (2007).
[61]G.-L. Oppo, M. Brambilla, and L. A. Lugiato, Phys. Rev. A **49**, 2028 (1994).
[62]S. Trillo, M. Haelterman, and A. Sheppard, Opt. Lett. **22**, 970 (1997).
[63]K. Staliunas, Phys. Rev. Lett. **81**, 81 (1998).
[64]G.-L. Oppo, A. J. Scroggie, and W. J. Firth, J. Opt. Soc. Am. B **1**, 133 (1999).
[65]D. V. Skryabin and W. J. Firth, Opt. Lett. **24**, 1056 (1999).
[66]P. Lodahl, M. Bache, and M. Saffman, Opt. Lett. **25**, 654 (2000).
[67]G.-L. Oppo, M. Brambilla, and L. A. Lugiato, Phys. Rev. A **63**, 023815 (2000).
[68]M. Tlidi, P. Mandel, M. Le Berre, E. Ressayre, A. Tallet, and L. di Menza, Opt. Lett. **25**, 487 (2000).
[69]M. Tlidi, D. Pieroux, and P. Mandel, Opt. Lett. **28**, 1698 (2003).
[70]M. Le Berre, E. Ressayre, and A. Tallet, Phys. Rev. E **67**, 066207 (2003).